Available online at www.sciencedirect.com
SCIENCE DIRECT®
International Journal of Heat and Mass Transfer 49 (2006) 2207–2214
International Journal of HEAT and MASS TRANSFER
www.elsevier.com/locate/ijhmt

Boiling propagation of water on a smooth film heater surface

Kunito Okuyama [a,*], Jeong-Hun Kim [b], Shoji Mori [a], Yoshihiro Iida [a]

[a] *Department of Chemical Engineering Science, Yokohama National University, 79-5 Tokiwadai, Hodogaya-ku, Yokohama, Kanagawa 240-8501, Japan*
[b] *Institute of Ocean Energy, Saga University, Yamashiromachi, Imari, Saga 849-4256, Japan*

Received 25 February 2005; received in revised form 14 November 2005
Available online 17 February 2006

Abstract

Boiling propagation of water is investigated experimentally at atmospheric pressure using a small platinum film heater having a surface smoothness of nanometer order. The test water is highly superheated up to approximately 140 K before the inception of boiling on the stepwise powered heater. Boiling is triggered at the prescribed wall superheat before spontaneous inception by generating a boiling bubble at a local section of the heater. The behavior of the propagating bubble is revealed by stroboscopic photography. The propagation takes place at wall superheats larger than approximately 50 K, and the propagation velocity increases significantly with wall superheat up to 24 m/s. The propagating front is followed by prompt collapse of the bubble at the tail, resulting in rapid migration of the boiling region. The measured propagation velocity is compared with the value predicted using an analytical model reported in the literature, and reasonable agreement is shown over the entire range of the wall superheat.

Keywords: Boiling propagation; Water; Small film heater; Bubble behavior; Propagation velocity

1. Introduction

When a highly-wetting liquid is heated on a solid surface, the wall superheat can reach the order of several tens of Kelvins before boiling incipience, and as soon as a few nucleation sites are activated, the boiling region extends quickly over the entire heated surface. For example, on a stepwise powered foil heater in saturated liquid nitrogen at atmospheric pressure, an initial bubble, which is generated at high wall superheat near the homogeneous nucleation temperature, grows into a hemispherical shape and simultaneously grows along the heated surface, resulting in a shape similar to a straw hat [1]. The bottom part continues to grow at an almost constant rate until its leading tip reaches the end of the heater length, whereas the growth of the hemispherical portion ceases when it extends to the heater width. A similar phenomenon has also been observed for other highly-wetting liquids, such as organic liquids [2–4], refrigerants [5–7] and a mixture of water and organic additives [8], as well as cryogenic liquids [9–11], on fine wires [2,4,9–11], films [6,8], foil heaters [5], metal tubes [3] and metal plates [7]. The bubble growth rate has a strong non-linear dependence on the wall superheat while being less dependent on the wall heat flux, and is also affected by the surface roughness, ranging from several tens of cm/s to several tens of m/s [1,3,7]. In refrigerant R113 boiling on a metal plate surface, the growth of the bottom part of the bubble was found to occur by the successive activation of bubble nuclei in the non-boiling region adjacent to the preceding nucleated bubbles and coalescence of these bubbles to give an increasingly larger bubble spreading out along the heated surface [7]. Since successive activation of the nuclei along the surface can be regarded as a kind of propagation phenomenon with respect to boiling nucleation, the above-described peculiar configuration has been referred to as boiling propagation or boiling front propagation. The distortion of the temperature field in the superheated liquid due to the growth of the preceding

* Corresponding author. Tel./fax: +81 45 339 4009.
E-mail address: okuyama@ynu.ac.jp (K. Okuyama).

0017-9310/$ - see front matter © 2006 Elsevier Ltd. All rights reserved.
doi:10.1016/j.ijheatmasstransfer.2006.01.001

Nomenclature

c_p	specific heat, J/(kg K)
h	heat transfer coefficient in liquid phase at the propagating front, W/(m^2 K)
i	enthalpy, J/kg
j	evaporative mass flux, kg/(m^2 s)
P	system pressure, Pa
Q	power per unit heater surface area, W/m^2
Q_{av}	time-averaged power per unit heater surface area, W/m^2
q_f	wall heat flux to liquid, W/m^2
r_2	radius of curvature of liquid–vapor interface at the propagating front, m
T_w	heater surface temperature, °C
T_l	liquid temperature, °C
ΔT_{sat}	wall superheat, K
$\Delta T_{sat,p}$	wall superheat at the onset of boiling propagation, K
$\Delta T_{sat,trig}$	wall superheat at triggering, K
t	time elapsed after onset of heating, s
v_f	liquid velocity at infinity, m/s
$V_{p,av}$	average velocity of boiling propagation, m/s
δ	film thickness, m
ρ	density, kg/m^3
σ	surface tension, N/m

Subscripts

0	liquid phase at propagating front
1	vapor phase at propagating front
∞	infinity

Superscripts

$''$	vapor
$'$	liquid

bubble may affect the induction of boiling in the adjacent region. However, the mechanism of the propagation has not yet been clarified.

Under highly subcooled conditions, the propagating bubble on a small heater surface grows as if a single bubble is migrating rapidly along the heater length, because the growth at the preceding portion is followed by collapse due to condensation [8]. Therefore, if boiling propagation is initiated from one end of the heater in a microchannel, of which both the height and width are approximately equal to those of the coalesced bubble, then the advancing growth of the bubble along the heated surface and the subsequent collapse thereof may cause a net liquid transport toward the propagating direction. Moreover, the repetition of boiling propagation at a prescribed frequency may enable continuous liquid transport by a single heater placed on a straight microchannel without any structure, such as nozzles or diffusers, which were used in many previous studies on micropumps using boiling bubbles. In previous studies [8,12], the authors demonstrated that boiling propagation repeated in the prescribed direction on a film heater placed along a U-shaped microchannel can provide continuous liquid transport. The configuration of propagation, propagation velocity and allowable repetition frequency were also investigated under pool boiling conditions at atmospheric pressure. The ink used in thermal inkjet printers, which is a relatively highly-wetting aqueous solution, was used as the test liquid, because prompt bubble collapse after the termination of heating is essential for the repetition of boiling propagation at higher frequencies, and, printer ink is responsive to heating repetition at high frequencies of approximately 10,000 Hz.

High incipient boiling wall superheat can be attained, even for water, by (a) increasing the heat load quickly, (b) heating at reduced ambient pressure, and/or (c) applying a heater having a very smooth surface. As for cases (a) and (b), which have been used extensively for water in conventional studies, the peculiar bubble growth similar to those in highly-wetting liquids was only observed under reduced (subatmospheric) pressure conditions [13]. More recent studies have been concerned with the phenomenon arising under the situation of case (c) or the situation of combining of cases (a) and (c), particularly as this regards application to micro-electro-mechanical systems (MEMS). In the present study, boiling propagation of water at atmospheric pressure is investigated using the small platinum film heater described in previous studies [8,12], the surface of which is smooth enough for liquid to be highly superheated before boiling incipience. Boiling is initiated on the heater immersed in a liquid pool and powered stepwise at an arbitrary prescribed wall superheat, which is lower than the wall superheat at spontaneous inception of boiling, by generating a triggering bubble at one end of the heater. The detailed bubble behavior during propagation, especially around the front of the propagating bubble, is revealed by stroboscopic photography through a microscope. The propagation velocity is compared with the prediction obtained by an analytical model reported in the literature, in which non-equilibrium evaporation during the disintegration of highly superheated liquid is considered to sustain the propagation.

2. Experimental apparatus and procedures

Fig. 1 shows a sketch of the test film heater. The film heater is produced by the evaporation deposition of titanium and platinum films, having thicknesses of 0.05 and 0.20 μm, respectively, onto a quartz glass substrate. The width and effective length of the heating section were 0.20 and 2 mm, respectively. Non-uniformity in the film thick-

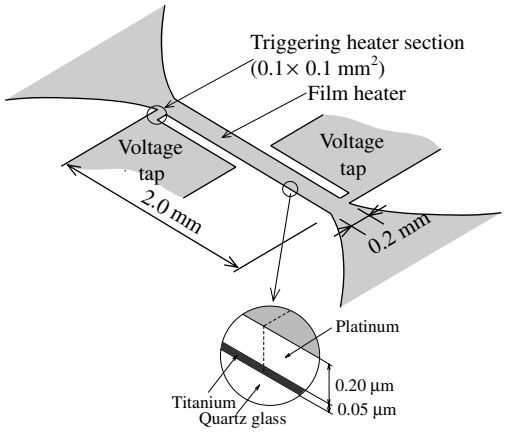

Fig. 1. Sketch of the test film heater.

ness over the effective length was less than ±2%, as determined by laser interferometry. The film surface was scanned by an atomic force microscope (AFM) at several locations. Fig. 2 shows the typical result of the AFM image. Although there is an unevenness of approximately 15 nm in height for each 50 nm along the surface, the surface is smooth and cavities by which to entrap gas or vapor as potential bubble nuclei are not likely to exist. The similar images were also obtained at different locations. Two voltage taps are prepared at both ends of the heating section, separated by a distance of 2 mm, to enable measurement of the average heater temperature by resistance thermometry during heating. The heater was exposed to a temperature of 350 °C for 13 h in a thermostatic bath before the boiling experiment in order to ensure that the temperature–resistance relationship of the composite film would be stable. The test specimen and composing materials were cleaned with trichloroethylene prior to setting up the test section. After setup, the test section was immersed in a small test-liquid-filled vessel with the heater surface facing the observation window. As the test liquid, commercially available distilled water of reagent grade, which was degassed by boiling for 3 h before the experiment, was used. The heater surface was also degassed simultaneously by boiling the test liquid by supplying a small pulse current in a short period at 1 Hz. After cooling the system, the experiment was conducted at atmospheric pressure and room temperature under pool boiling conditions.

Fig. 3 shows a schematic diagram of the experimental apparatus. A rectangular pulse heating signal from a pulse generator was amplified by a power amplifier. The film heater was powered stepwise for a short duration by the current from the amplifier (see the "Main" circuit in Fig. 3). The voltage difference between the two voltage taps and the voltage difference corresponding to the heating current at a standard resistance inserted in the heating circuit were recorded using a digital oscilloscope and the heating power was calculated. The power decreases slightly with time before boiling incipience as the heater temperature, and consequently, the electrical resistance, increase due to the heat generation. The average heater temperature between the taps in the heating section was obtained by referencing the measured electrical resistance to a calibration curve, which was carefully obtained in the temperature range of interest using a thermostatic bath. A standard platinum resistance thermometer was attached securely to the specimen in the bath. In order to confirm the accuracy of the temperature measurement during the stepwise heating, one-dimensional transient heat conduction calculations

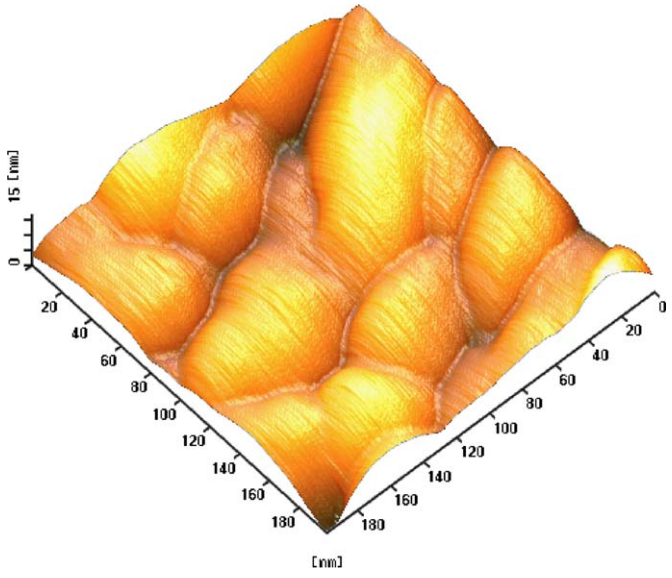

Fig. 2. Test platinum film surface scanned by atomic force microscope (AFM).

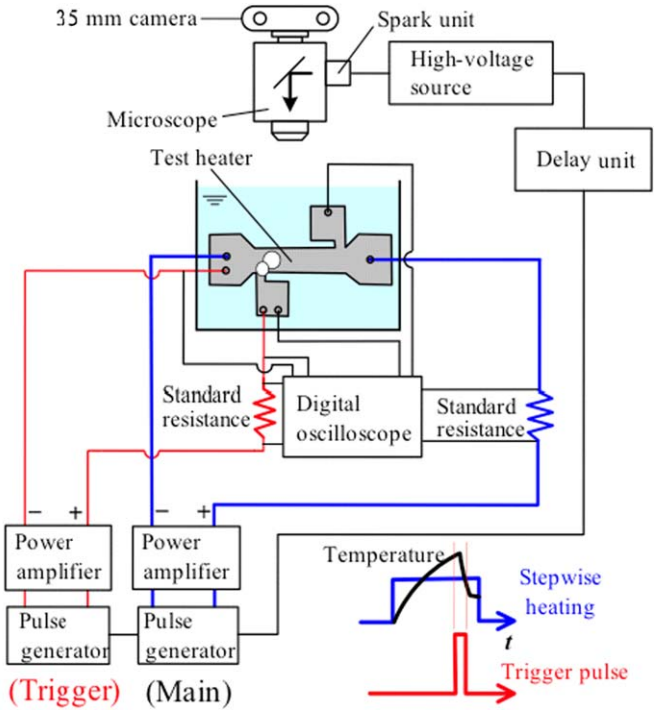

Fig. 3. Schematic diagram of the experimental apparatus.

for a liquid-heater-quartz glass system were carried out assuming the properties of liquid water. The temperature difference across the heater film thickness was less than 0.1 K, even at the maximum heating power. The measured average temperature can therefore be regarded as the average surface temperature, and also as the temperature of the liquid in contact with the heater surface. The uncertainty in the measurement of the average heater temperature was estimated to be within ±7 K. This is attributed to the uncertainty in measuring the voltage difference and current (±6 K) and the uncertainty in expressing the resistance as a function of temperature by a polynomial (±1 K). The local film temperature difference due to the non-uniformity of the film thickness is estimated to be within ±14 K. In addition to the liquid temperature or superheat at the heated surface, the heat flux q_f transferred to the fluid (the wall heat flux) is an important parameter in characterizing the transient boiling phenomena during the stepwise heating. The wall heat flux can be obtained by subtracting from the heating power per unit heating area the conduction heat flux q_{qg} transferred to the quartz substrate and the heat storage rate in the heater film, following the energy balance equation:

$$q_f(t) = Q(t) - q_{qg}(t) - \left\{(c_p\rho\delta)_{Pt} + (c_p\rho\delta)_{Ti}\right\}\frac{dT_w}{dt}, \qquad (1)$$

where q_{qg} was calculated from the numerical solution of the one-dimensional transient heat conduction equation for a semi-infinite medium (quartz glass) by using the measured time sequence of the film temperature as a boundary condition. The time-averaged value of the wall heat flux to the liquid from the onset of heating to boiling incipience was estimated to be approximately 52% of the heating power for water.

The boiling process on the heater was photographed through a microscope at ×25 magnification using a 35-mm camera and 10-ns pulse stroboscopic lighting. The timing of the lighting (one flash per stepwise heating) was adjusted using a delay unit triggered by the onset of heating. As described in detail in the following paragraph, boiling on the heater was triggered at the prescribed timing during the stepwise heating in all experiments except for the measurement of the wall superheat at the spontaneous inception of boiling without triggering. The time sequence from bubble generation to collapse was recorded by changing the timing of the lighting. An ISO 3200 film was used and sensitized during development so as to be equivalent to ISO 25000. This observation system provided sufficiently high resolution to observe clearly the boiling propagation process on the heater surface at a high speed of over 10 m/s. A high-speed video camera, with a frame rate of 18,000 frames/s and an exposure period per frame of 5 μs, and a 150-W metal halide lamp were used to measure the time of boiling incipience and the propagation velocity during the stepwise heating without triggering boiling, although the resolution was not sufficient. The video recording was triggered by starting the stepwise heating.

In order to capture clearly the boiling sequence using the current photographic observation system, the boiling phenomena are required to take place with high reproducibility under prescribed conditions for each stepwise heating. In addition, it is desirable that the wall superheat at the inception of boiling can be adjusted to an arbitrary prescribed value as the experimental parameter. Therefore, a special technique was used in the present study. For each stepwise heating period, a boiling bubble was rapidly generated at the converged fine tip (having an area of 0.1 mm × 0.1 mm) (see triggering heater section in Fig. 1) of the voltage tap at the prescribed end of the heater via an additional short, intense (approximately 100 MW/m^2) pulse (of width 0.1 ms) supplied from an alternative heating circuit (see the triggering circuit in Fig. 3). Boiling on the heater was triggered by this bubble. The timing of the triggering, that is, the duration from the onset of heating the entire heater surface to the triggering at the tap, was set such that boiling and/or propagation were initiated on the heater when its average temperature during the stepwise heating approached a prescribed wall superheat before the spontaneous inception of boiling. The duration was determined from the measured time variation of the heater temperature during stepwise heating. Each stepwise heating power was turned off immediately after the completion of the propagation over the heater length.

3. Experimental results and discussion

Figs. 4 and 5 show photographs just subsequent to boiling incipience of distilled water and the corresponding time traces of the wall superheat, respectively, at the stepwise power of $Q_{av} = 12.5$ MW/m^2. The time traces of the heating power Q and the heat flux q_f transferred to the fluid were also shown in Fig. 5. Here, Q_{av}, t, T_w and ΔT_{sat} denote the time averaged stepwise power from the onset of heating to boiling incipience, the time elapsed after the onset of heating, the heater surface temperature and the wall superheat, respectively. Wall superheat was defined as the temperature difference between the wall temperature and the saturation temperature of water at atmospheric pressure. The average rate of the heater temperature increase up to boiling incipience was approximately 10^5 K/s, and the wall superheat at boiling incipience without triggering ranged from approximately 115–140 K, which is still considerably lower than the superheat corresponding to homogeneous nucleation (approximately 200 K). Three cases of wall superheat at triggering for boiling initiation, $\Delta T_{sat,trig} = 70$, 90 and 110 K, which are lower than that of the spontaneous inception, are shown in the figures. The triggering bubble was generated by the additional heating pulse at the narrow tip of the voltage tap at the left end of the heater when the heater temperature increased up to the prescribed high wall superheat. As soon as boiling was induced on the heater surface adjacent to the tap, boiling propagated quickly toward the opposite end of the effectively heated region. The activation of bubble

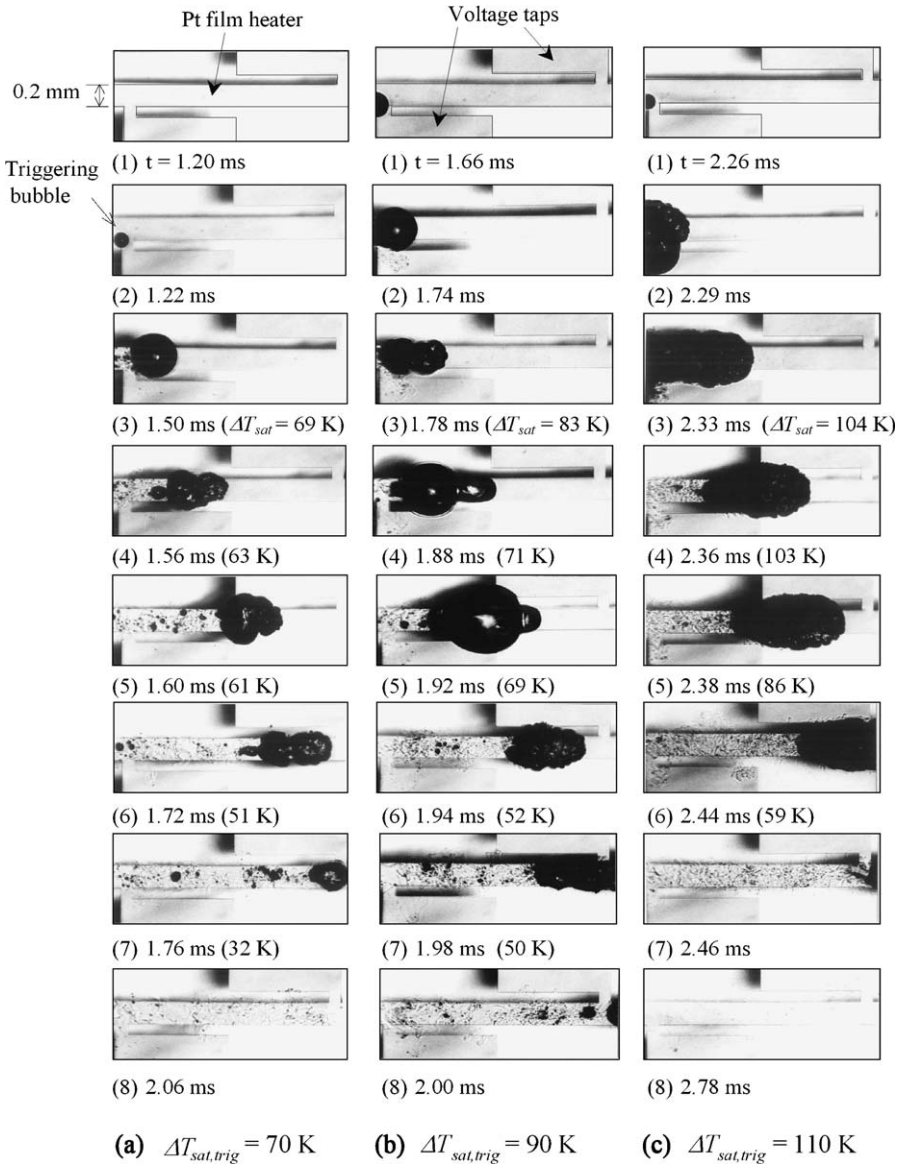

Fig. 4. Boiling propagation of distilled water triggered on a platinum film heater powered stepwise under pool boiling conditions ($T_\ell = 25$ °C, $Q_{av} = 12.5$ MW/m^2).

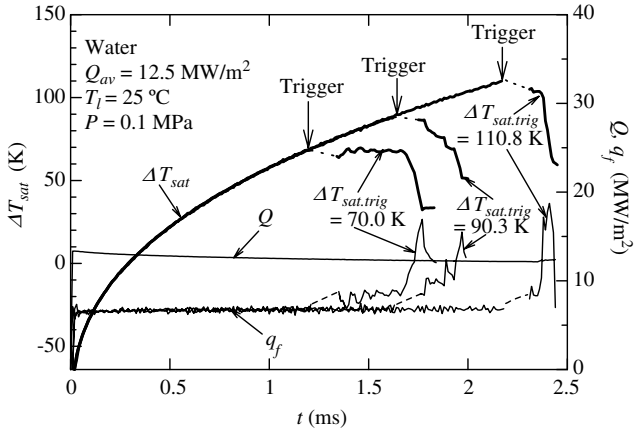

Fig. 5. Time traces of the wall superheat and heat flux to fluid during stepwise heating corresponding to the photographs in Fig. 4.

nuclei in the non-boiling region adjacent to the preceding nucleated bubbles and rapid coalescence growth exceeding the heater width can be observed clearly (see frames (4) and (5) at $\Delta T_{sat,trig} = 90$ K). The propagation is followed by the prompt collapse of the bubble at the tail, resulting in rapid migration of the boiling area along the heated surface. The migrating boiling area and the propagation velocity tend to increase as the wall superheat at the triggering is increased. The distorted contour of the boiling area and the awkward migration, as seen in Fig. 4(a) and (b), may be due to the irregular induction of nucleation around the propagating front. As the boiling area approaches the opposite end, the wall superheat decreases significantly due to the augmented heat transfer, to approach that of steady-state boiling (approximately 30–40 K). (During the triggering pulse period, the heater temperature cannot be measured because

of the superposition of the triggering current to the "Main" circuit.) The heat flux to the fluid exceeds temporarily the heating power. A similar configuration was observed in the range of $\Delta T_{sat,trig}$ from 40 to 110 K. The configuration of the boiling propagation does not appear to differ greatly from those for highly-wetting liquids observed in conventional studies [1–7] or from those for ethyl alcohol and ink-jet printer ink examined using the same platinum film heater by the authors in previous reports [8,12].

Without triggering, the incipient boiling wall superheat for water was higher than 110 K. Such high incipient superheat, which corresponds to a critical bubble radius smaller than 70 nm according to the Laplace equation and the Clausius–Clapeyron equation, may be due to the significant smoothness of the current film heater surface as produced by evaporation deposition. As described in the preceding section, boiling propagation at atmospheric pressure has not yet been reported for water. The boiling surfaces in conventional studies, using wires, foils, plates or blocks of metals, have roughness due to mechanical machining or polishing, and in these cases, the incipient boiling wall superheat is not high enough for water. The current film surface has sufficient smoothness to cause incipient boiling superheat to adequately induce boiling propagation even in water. The boiling propagation may not be limited to highly-wetting liquids, but may also occur for other liquids if the surface conditions of the solid can enable the incipient boiling superheat to be much higher than the superheat at steady-state boiling.

In a previous report [12], top- and side-view photographs of boiling for the ink-jet printer ink on the platinum film heater of the present experiment were taken under the same conditions of heating power and wall superheat at the triggering as those for distilled water in Fig. 4. The printer ink, having a surface tension of 43 mN/m (at room temperature), which is much lower than that of pure water, and the main ingredients, consisting of water (>80%), ethylene glycol and isopropyl alcohol, were supplied without adding dye to visualize the boiling bubbles. The configuration of the propagation was unexpectedly similar to that for distilled water (shown in Fig. 4), i.e., rapid propagation along the heated surface and subsequent collapse of the bubble at the tail, resulting in rapid migration of the boiling area. The propagation velocity was slightly lower than that of water at the same wall superheat and increased with the wall superheat in manner similar to that of water. The side view showed that the front of the propagating bubble of approximately 0.2 mm in height was smooth and wedge-like, whereas the collapsing rear end showed significant distortion and/or fluctuation [12].

Fig. 6 shows the average propagation velocity $V_{p,av}$ for distilled water plotted with respect to wall superheat at the onset of propagation $\Delta T_{sat,p}$ as measured by changing the wall superheat at $\Delta T_{sat,trig}$. The propagation velocities without triggering are also plotted in the figure. The average propagation velocity is defined as the propagation distance divided by the corresponding period from the onset

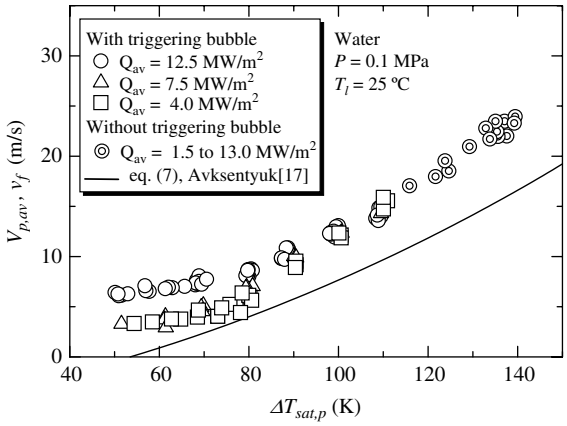

Fig. 6. Average propagation velocity $V_{p,av}$ plotted with respect to wall superheat at propagation $\Delta T_{sat,p}$ measured by changing the wall superheat at triggering $\Delta T_{sat,trig}$.

of propagation to the arrival of the propagating front to the end of the heating section. Under triggering, boiling propagation occurred with a slight delay after the generation of the triggering bubble for $\Delta T_{sat,trig}$ lower than approximately 80 K. Therefore, $\Delta T_{sat,trig}$ is not always equal to $\Delta T_{sat,p}$. The delay may depend on the process of the activation or site-seeding for the bubble nucleus in the heater region by the bubble generated in the adjacent triggering heater section. $\Delta T_{sat,p}$ which represents the wall superheat at propagation was chosen as the abscissa in the figure. When the propagation started during the triggering pulse period, $\Delta T_{sat,p}$ was obtained by interpolation between the temperatures before and after the triggering pulse. The propagation occurred only at wall superheats larger than approximately 50 K, and $V_{p,av}$ increased significantly with the increase in $\Delta T_{sat,p}$, to approach the velocity for the case without triggering bubbling. The velocity was less dependent on the stepwise heating power, and was therefore less dependent on the wall heat flux to fluid, except at superheats lower than 80 K. The larger average velocity at the higher heating power at lower superheats is due to the significant increase in the heater temperature in the non-boiling region during the propagation and the resulting increase in the propagation velocity. The existence of the threshold value for wall superheat, below which propagation does not occur, and the significant increase in the propagation velocity with wall superheat above this threshold are similar to the results for highly-wetting liquids [1,7,14]. The advance of the propagating front was somewhat awkward at $\Delta T_{sat,p}$ below 90 K and became smoother (with constant velocity) at high wall superheats over 100 K. For several organic liquids, the propagating front is reported to change from slow to fast propagation at a particular wall superheat, resulting in a jump in the propagation velocity [14,15]. Although the propagation velocity increases monotonously with the wall superheat for water in the present experiment, there may be two different modes for boiling propagation, i.e., (a) distinct activation of bubble nuclei in the region adjacent to the

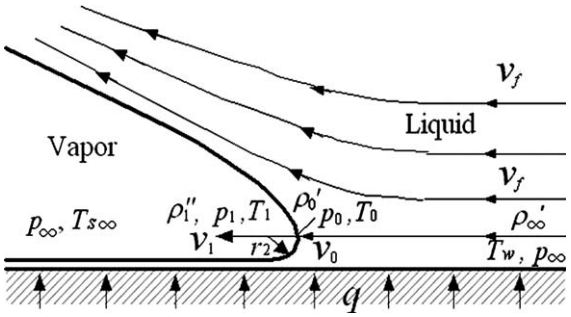

Fig. 7. Liquid and vapor flow around the front of the propagating bubble.

propagating front and coalescent growth of nucleated bubbles and (b) smooth advance of the propagating front along the heated surface.

For the smooth advance of the propagating front, several models have been proposed in order to predict the propagation velocity [3,16–18]. Avksentyuk [3,16,17] assumed that the recoil force corresponding to the evaporative momentum flux emerging from the liquid–vapor interface due to the disintegration of the superheated liquid layer balances the dynamic pressure arising in the liquid phase at the front of the propagation layer advancing along the heated surface. A moving coordinate system was introduced as shown in Fig. 7, where the propagating front is motionless and liquid flows from the right to the front and vapor moves to the left from the evaporation surface. The equations of mass, momentum and energy flux conservations through the evaporation surface at the propagating front are expressed as

$$j = \rho_0' v_0 = \rho_1'' v_1, \tag{2}$$

$$p_0 + \rho_0' v_0^2 = p_1 + \rho_1'' v_1^2 - \frac{\sigma_0}{r_2}, \tag{3}$$

and

$$j(i_1 - i_0) = h(T_w - T_0), \tag{4}$$

respectively, where j is the evaporative mass flux, ρ is the density, σ is the surface tension, i is the enthalpy, and h is the heat transfer coefficient at the propagating front in the liquid phase. In addition, the single prime denotes a liquid and the double prime denotes a vapor. The subscript "0" refers to the values at the liquid–vapor interface in the liquid, and the subscript "1" refers to the values in vapor on the outer border of the Knudsen layer at the liquid–vapor interface.

The motion equation for liquid was reduced to the Bernoulli's equation under the non-viscous approximation. Between the free flow and the propagating front, we therefore have

$$p_0 + \frac{\rho_0' v_0^2}{2} = p_\infty + \frac{\rho_\infty' v_f^2}{2}. \tag{5}$$

Under the assumption that the vapor pressure force is equal to the capillary force at the propagating front [17], the main curvature radius at the front was determined from

$$r_2 = \frac{\sigma_0}{(p_1 - p_\infty)}. \tag{6}$$

From Eqs. (2), (3), (5) and (6), at $\rho_1'' \ll \rho_0'$, the propagation velocity is given by

$$v_f = j\sqrt{\frac{2}{\rho_1'' \rho_\infty'}}. \tag{7}$$

The theory of non-equilibrium evaporation from the superheated liquid, which was derived from the kinetic theory of gases, was employed for the estimation of the evaporative mass flux. The relation for j derived by Labuntsov and Kryukov [19] was used. The heat transfer coefficient in the liquid phase around the propagating front was approximated as that in the vicinity of the stagnation point of a cylinder, the radius of which is equal to the main curvature radius of the propagating front, placed in a non-viscous liquid. In the calculation, the value of the liquid temperature at the liquid–vapor interface T_0 was assumed and then corrected iteratively until the value of the propagation velocity to satisfy all equations will be obtained. The solid line in Fig. 6 represents the prediction by the model of Avksentyuk [17]. Although the estimated values of velocity are slightly lower than those measured at the same wall superheat, the model expresses well the threshold and the dependency of the measured velocity on the wall superheat over the entire superheat range. The calculated heat transfer coefficient in liquid phase h and evaporative mass flux j at the propagation front are approximately 0.9, 4.8 and 12 MW/(m^2 K) and 24, 150 and 450 kg/(m^2 s) for the wall superheats $\Delta T_{sat} = 65$, 100 and 145 K, respectively. The theoretical values of the propagation velocity may change somewhat depending on the relationships used to estimate the evaporation mass flux in the non-equilibrium state and on the relationships for the heat transfer coefficient in the liquid phase. With the increase of 10% in h, the propagation velocity increases by 20% at $\Delta T_{sat} = 90$ K, and with the increase of 10% in j, the propagation velocity increases by 5% at the same wall superheat. The calculated temperature of the liquid–vapor interface at the propagating front T_0 is plotted with respect to the wall superheat in Fig. 8, together with the wall temperature T_w, as a reference. The wall superheat in the figure is the difference between the wall temperature and the saturation temperature at atmospheric pressure. Here, T_0 is considerably lower than the wall temperature and begins to increase significantly with the wall superheat at approximately 55 K. The difference in T_0 from the saturation temperature T_{sat} becomes significant and comparable to the difference between T_w and T_0 at higher wall superheats. This implies that the interfacial resistance for the evaporation associated with the molecular kinetics may have a significant influence on the evaporation rate, and therefore on the propagation velocity, at higher wall superheats. Further examination of the models is needed in order to further clarify the

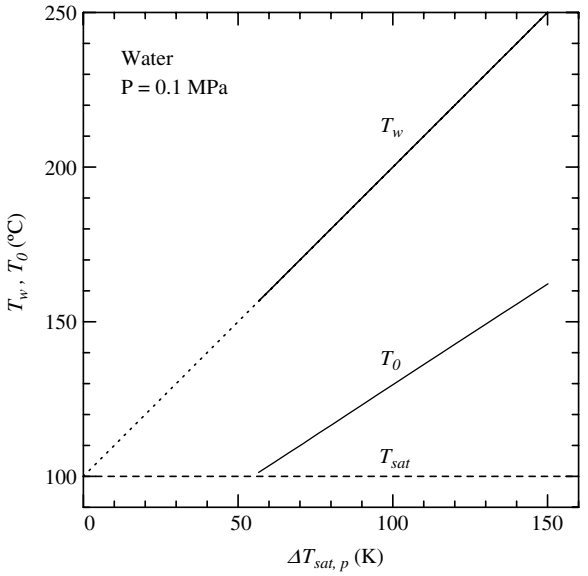

Fig. 8. Calculated temperature of the liquid–vapor interface at the propagating front T_0 plotted with respect to wall superheat.

mechanism for sustaining propagation. In particular, it is necessary (a) to clarify the relationship among the vapor pressure outside the Knudsen layer, the evaporative momentum flux, the capillary force and the saturation vapor pressure on the liquid–vapor interface at the propagating front, (b) to derive a more appropriate heat transfer coefficient in the liquid phase, and (c) to take into account the influence of liquid subcooling. The activation mechanism of the bubble nucleus in the region adjacent to the propagating front and its criteria should also be clarified.

4. Conclusions

The configuration of boiling propagation of distilled water on a small platinum film heater has been investigated at atmospheric pressure. Boiling was initiated on a stepwise powered heater at the prescribed wall superheat by generating a triggering bubble at the end of the heater. Boiling propagation was shown not only to occur for highly-wetting liquids but also to occur even for water at atmospheric pressure when the heater surface is sufficiently smooth so that the wall superheat at the boiling incipience becomes much higher than that of steady-state boiling. The propagation in subcooled water was followed by the prompt collapse of the bubble at the tail, resulting in rapid migration of the boiling area along the heated surface. The existence of a threshold value for wall superheat under which the propagation does not appear and the significant increase in the propagation velocity with the wall superheat were similar to the results reported for various liquids and heaters in previous reports. The propagation velocity predicted by the model reported in the literature agreed reasonably with the measured results. Non-equilibrium evaporation was shown to be significant for the propagation.

Acknowledgement

This study was supported in part by a Grant-in-Aid from the Japan Society for the Promotion of Science (No. 13555053).

References

[1] K. Okuyama, Y. Iida, Premature transition to film boiling at stepwise heat generation, Heat Transfer Jpn. Res. 21 (3) (1992) 317–329.
[2] M. Sako, H. Kanamaru, Y. Kikuchi, Bubble behavior and transient heat transfer at inception of boiling, 27th National Heat Transfer Symp. Japan 1 (1990) 307–309 (in Japanese).
[3] B.P. Avksentyuk, V.V. Ovchinnikov, V.Ya. Plotnikov, Dynamic effects on interphase surface during the disintegration of superheated near-wall liquid, in: Proc. Int. Cent. Heat Mass Transfer, vol. 33, No. Phase-Interface Phenom. Mulfronthase Flow, 1991, pp. 583–598.
[4] K. Okuyama, Y. Iida, H. Sasaki, J.H. Kim, Vapor generation and collapse behavior on a fine wire subjected to pulse heating (experimental results for a wide range of heating rates), Thermal Sci. Eng. 7 (4) (1999) 37–43.
[5] K. Okuyama, Y. Kozawa, A. Inoue, S. Aoki, Transient boiling heat transfer characteristics of R113 at large stepwise power generation, Int. J. Heat Mass Transfer 31 (10) (1988) 2161–2174.
[6] J.S. Ervin, H. Merte Jr., R.B. Keller, K. Kirk, Transient pool boiling in microgravity, Int. J. Heat Mass Transfer 35 (3) (1992) 659–674.
[7] K. Okuyama, Y. Iida, T. Kato, Premature transition to film boiling at stepwise heat generation, 2nd Report: Effect of wall material and surface condition, Heat Transfer Jpn. Res. 25 (1996) 51–63.
[8] K. Okuyama, R. Takehara, J.H. Kim, Y. Iida, Micropump using boiling propagation phenomena, Thermal Sci. Eng. 10 (4) (2002) 19–20.
[9] O. Tsukamoto, T. Uyemura, Observation of bubble formation mechanism of liquid nitrogen subjected to transient heating, Adv. Cryog. Eng. 25 (1980) 476–482.
[10] A.N. Pavlenko, V.Yu. Chekhovich, Burn-out heat transfer in unsteady state heat generation in a cryogenic fluid, Heat Transfer Sov. Res. 18 (3) (1986) 83–94.
[11] K. Okuyama, Y. Iida, Transient boiling heat transfer characteristics of nitrogen (bubble behavior and heat transfer rate at stepwise heat generation), Int. J. Heat Mass Transfer 33 (10) (1990) 2065–2071.
[12] K. Okuyama, J.H. Kim, R. Takehara, Y. Iida, Pumping action by boiling propagation in a microchannel, Microscale Thermophys. Eng. 9 (2005) 119–135.
[13] B.P. Avksentyuk, V.V. Ovchinnikov, A study of vapor formation structure in water at high superheating, heat and mass transfer in chemical process industry accidents, in: Proc. Int. Symp., Rome, 1994, pp. 275–283.
[14] J. Mitrovic, J. Fauser, Propagation of boiling fronts along horizontally arranged heated tubes, Trans. Inst. Chem. Eng. 79 (Part A) (2001) 363–370.
[15] S.A. Zhukov, V.V. Barelko, Dynamic and structural aspects of the processes of single-phase convective heat transfer metastable regime decay and bubble boiling formation, Int. J. Heat Mass Transfer 35 (4) (1992) 759–775.
[16] B.P. Avksentyuk, V.V. Ovchinnikov, A study of evaporation structure at high superheatings, Russian J. Engng. Thermophys. 3 (1993) 21–39.
[17] B.P. Avksentyuk, Non-equilibrium model of an evaporation front, Russ. J. Eng. Thermophys. 5 (1995) 1–8.
[18] A.N. Pavlenko, V.V. Lel', Model of self-maintaining evaporation front for superheated liquids, in: Third Int. Conf. Mulfronthase Flow, ICMF'98, Lyon, France, June 8–12, 1998.
[19] D.A. Labuntsov, A.P. Kryukov, Analysis of intensive evaporation and condensation, Int. J. Heat Mass Transfer 22 (1979) 989–1002.